



LAWRENCE
LIVERMORE
NATIONAL
LABORATORY

Pressure Dependent Decomposition Kinetics of the Energetic Material HMX up to 3.6 GPa

E. A. Glascoe, J. M. Zaug, A. K. Burnham

June 1, 2009

Journal of Physical Chemistry A

Disclaimer

This document was prepared as an account of work sponsored by an agency of the United States government. Neither the United States government nor Lawrence Livermore National Security, LLC, nor any of their employees makes any warranty, expressed or implied, or assumes any legal liability or responsibility for the accuracy, completeness, or usefulness of any information, apparatus, product, or process disclosed, or represents that its use would not infringe privately owned rights. Reference herein to any specific commercial product, process, or service by trade name, trademark, manufacturer, or otherwise does not necessarily constitute or imply its endorsement, recommendation, or favoring by the United States government or Lawrence Livermore National Security, LLC. The views and opinions of authors expressed herein do not necessarily state or reflect those of the United States government or Lawrence Livermore National Security, LLC, and shall not be used for advertising or product endorsement purposes.

Pressure Dependent Decomposition Kinetics of the Energetic Material HMX up to 3.6 GPa

Elizabeth A. Glascoe,^{} Joseph M. Zaug, and Alan K. Burnham*

Lawrence Livermore National Laboratory, 7000 East Avenue, Livermore, California 94551

AUTHOR EMAIL ADDRESS glascoe2@llnl.gov

RECEIVED DATE (to be automatically inserted after your manuscript is accepted if required according to the journal that you are submitting your paper to)

^{*} To whom correspondence should be addressed: E-mail: glascoe2@llnl.gov

ABSTRACT

The effect of pressure on the thermal decomposition rate of the energetic material HMX was studied. HMX was precompressed in a diamond anvil cell (DAC) and heated at various rates. The parent species population was monitored as a function of time and temperature using Fourier transform infrared (FTIR) spectroscopy. Decomposition rates were determined by fitting the fraction reacted to the extended-Prout-Tompkins nucleation-growth model and the Friedman isoconversional method. The results of these experiments and analysis indicate that pressure accelerates the decomposition at low to moderate pressures (i.e. between ambient pressure and 1 GPa) and decelerates the decomposition at higher pressures. The decomposition acceleration is attributed to pressure enhanced autocatalysis whereas the deceleration at high pressures is attributed pressure inhibiting bond homolysis step(s), which would result in an increase in volume. These results indicate that both β and δ phase HMX are sensitive to pressure in the thermally induced decomposition kinetics.

KEYWORDS

HMX, Energetic Materials, High Pressure, Thermal Decomposition, Kinetics

Introduction

The role of pressure in the thermal decomposition mechanisms and kinetics of solid state energetic materials is an interesting and important topic. Pressure can accelerate heterogeneous and gas-phase reactions and can inhibit reactions that involve an increase in volume. Such competing effects make it difficult to predict the role of pressure without a detailed knowledge of the decomposition mechanism of a material. The pressure-dependent kinetics of thermal decomposition are of great importance to the assessment and prediction of thermal-safety of energetic materials, as pressure is a dynamic variable in any sealed container that is heated. This work describes pressure-dependent kinetics of the thermal decomposition of the energetic material, HMX (1,3,5,7-tetranitro-1,3,5,7-tetrazocane) between ambient pressure and 3.6 GPa.

HMX has been studied and used in a wide range of explosives and propellants for at least 60 years, hence, there is a solid foundation of literature describing its thermal decomposition mechanisms. Most studies indicate that the decomposition begins with either N-NO₂ bond homolysis or HONO formation although other initiation mechanisms have been observed.¹⁻⁴ The initial products of HMX decomposition attack the starting material and intermediates, producing a variety of autocatalytic reactions.^{3,4} The mechanisms and kinetics of HMX decomposition are described, in detail, in the literature.¹⁻¹¹

Although many aspects of the HMX decomposition mechanism are established, the effect of pressure is poorly understood. There exist only a few kinetic studies of solid state HMX decomposition, at elevated pressures, and a comparison of the results raises many questions. Burnham et al. monitored the decomposition of HMX using differential scanning calorimetry (DSC) between ambient pressure and 1000 psi (7E-3 GPa) and found that HMX decomposition accelerates as a function of pressure.⁸ However, Piermarini et al. found exactly the opposite trend when HMX was decomposed at higher pressures (ca. 3 – 6 GPa) in a diamond anvil cell (DAC).⁹ There are two major differences between these two studies, which might explain the contradicting trends: the polymorph of HMX which decomposes and the method of monitoring the decomposition. In Burnham's DSC results, HMX

decomposed from the δ -phase and is monitored via the heat flow produced from the chemical reactions. In Piermarini's DAC experiments, HMX decomposed from the β -phase and the population of HMX is monitored directly using FTIR spectroscopy. Based on these two studies, it is unclear what role pressure plays in the decomposition of HMX and whether the polymorph of HMX affects the decomposition rate.

Previous studies have provided limited insight into the role of the polymorph in the decomposition or deflagration of HMX. Pressure dependent deflagration studies up to several hundred MPa report that plastic-bonded-explosives burn much faster after undergoing a $\beta \rightarrow \delta$ phase transition.¹² However, the most likely reason for this acceleration in deflagration is improved penetration of the decomposition flame into cracks caused by the volume expansion during the $\beta \rightarrow \delta$ transition. Slow cook-off thermal explosion experiments provide no consistent trend from one material to the next concerning the violence of β versus δ -phase explosives.¹³ However, these cook-off experiments have multiple variables that can influence the reaction, making isolation of a polymorph variable difficult or impossible. Isothermal heating time-to-explosion studies indicate that raising the pressure from 1 to 5 GPa increases the explosion time by a factor of 3.¹¹ This result is qualitatively consistent with Piermarini et al.'s findings⁹ but quantitatively different, most likely due to the methods of detection and the more complex thermal transport mechanisms involved in a thermal explosion versus a thermal decomposition.

In this work, the decomposition kinetics of HMX are studied from ambient pressure up to 3.6 GPa through the combination of diamond anvil cell techniques and Fourier transform infrared spectroscopy (FTIR). By studying the kinetics at pressures identical to both Burnham et al.⁸ and Piermarini et al.⁹, as well as pressures that span between the two regimes, the opposing trend of the DSC and DAC results is resolved. The role of the HMX-polymorph is explored and the pressure-dependent kinetics of HMX decomposition are reported.

Experimental

Sample

HMX powder, manufactured by Holston Army Ammunition Plant (Hol 6HBFC21-25. LLNL number B-881), was reduced to a grain size of ca. 3 μm via fluid energy milling at Lawrence Livermore National Laboratory. In all experiments, HMX powder was sandwiched between cesium iodine (CsI) windows and packed into a DAC sample chamber. The CsI protected the diamonds from highly reactive decomposition products and transmitted applied pressure. Strontium tetraborate was used as a pressure manometer¹⁴ and was placed between the CsI window and the diamond culets so as to avoid chemical reactions with the decomposing HMX. The DAC sample cavity consisted of two counter-opposed 400 μm diameter, type II diamond culets and a pre-indented 50-70 μm thick Incanel foil gasket. The chamber diameter is cut using a micro-electric discharge machine (Hylozoic Products) and is nominally 100 μm .

Instrument

The decomposition of HMX was monitored in-situ via Fourier Transform IR spectroscopy (FTIR). The FTIR instrument was specially designed and built in-house in order to achieve the high spatial resolution necessary for monitoring small samples within the DAC; a detailed description of the instrument is described previously.¹⁵ Briefly, a mid-IR glowbar source is focused to a diameter of ca. 1 mm, transmitted through a sample, and focused into a cryogenically cooled single element InSb-HgCdTe sandwich detector. Two irises are situated along the beam path before and after the sample to enable $> 30 \mu\text{m}$ spatially resolved IR absorption measurements; however, in these experiments we typically filled the entire sample chamber in order to increase our signal to noise ratio. A Bruker Optics Vector 33 interferometer is used to collect 2 cm^{-1} resolution data between 400 and 5000 cm^{-1} . When averaging 15 interferograms, the instrument response time is approximately 1 min, and consequently only the kinetics of parent molecule depletion and final product formation were monitored. Background spectra of the diamond and CsI window material were collected prior to loading samples.

Decomposition Experiments

The sample was heated via a resistive heater ring (Watlow) attached to the outer circumference of the DAC. The cell temperature was monitored with a K-type thermocouple mounted at the diamond table. Thermal calibration of the sample temperature was roughly established by comparing the temperature of a thermocouple mounted on the interior diamond facet with the thermocouple measurements at the diamond table. The temperature readings at the two locations varied linearly with the heater temperature and at the highest temperature studied (320 °C) they differed by 22 °C. Fine calibration of the temperature disparity between the sample and the diamond table thermocouple was determined by comparing the HMX polymorph transformation (i.e. $\beta \rightarrow \delta$) temperature measured in the DAC and that measured using DSC at the same ramp rate. Fine calibration resulted in an additional adjustment of 8 °C at the highest temperatures (ca. 350 °C). Thermal ramping was controlled using a high stability temperature and process control unit (Eurotherm 2400 series).

In a typical experiment, HMX and CsI were loaded into the DAC and uniaxially compressed to a target pressure. The DAC was mounted into the heating ring and aligned to the FTIR microscope. In the isothermal experiments the sample was rapidly heated to the desired temperature and held constant. In the thermal ramp experiments the sample was rapidly heated to a moderate temperature (135 -170 °C depending on the pressure), allowed time to equilibrate (ca. 10 minutes), and heated further at a rate of either 0.5 or 0.25 °C/min. During the temperature equilibration period and periodically during the ramped heating phase the sample pressure was monitored and adjusted, in situ, as needed to maintain a constant pressure throughout each experiment.

Pressure was determined via the calibrated fluorescence wavelength shift of strontium tetraborate and maintained, in situ, with the use of a gas-actuated metal-membrane attached to the DAC. All experiments at $P \geq 1$ GPa were maintained at a constant pressure to within ca. 0.1 GPa prior to decomposition. During decomposition the pressure increased by ca. 0.40 GPa, presumably, due to formation of product gases. In the ambient pressure experiments, a small void was left between the

diamond and the CsI to allow for gas expansion without a pressure rise. No pressure measurements were made for the ambient pressure experiments; instead the temperature for the $\beta \rightarrow \delta$ transition was used to verify ambient pressure conditions. The reported pressures in the experiments between 0 and 1 GPa were estimated based on limited pressure measurements and the $\beta \rightarrow \delta$ transition temperature.¹⁶

Results

Spectral Analysis

Figure 1 shows the infrared spectrum of HMX at 3.6 GPa between 233.9 and 295.2 °C during a 0.5 °C/min ramp. HMX peak assignments are provided in the literature.¹⁷ At this pressure, the $\beta \rightarrow \delta$ transition is inhibited⁹; consequently, HMX is observed to decompose completely in the β -phase and no δ -phase HMX is observed. All the experiments at $P \geq 1$ GPa display similar spectral evolution and HMX is observed to decompose from the β -phase. Figure 2 shows the spectral evolution of the HMX asymmetric CH_2 stretch at ambient pressure between 178.4 and 186.1 °C. Here the change in peak position and profile between β and δ phase HMX is evident. The peak amplitude for each polymorph is plotted as a function of temperature in Figure 3; it is clear that at ambient pressure (and slow heating rates) β -HMX undergoes complete transformation to δ -HMX prior to decomposition. Experiments conducted at pressures between ambient pressure and 1 GPa show some β -phase decomposition prior to, and during, the $\beta \rightarrow \delta$ phase transformation.

In all the experiments, the peak amplitude for the CH_2 asymmetric stretch was used to monitor the population of HMX as a function of temperature. As a proof of principle, the HMX population was monitored using a variety of peaks in the lower wavenumber region of the spectrum and the decomposition rate was nearly identical for all peaks. Due to spectral congestion, these lower wavenumber peaks are more difficult to isolate, especially when both β and δ phase HMX are present. Consequently, the asymmetric CH_2 stretch was used to monitor all the HMX decompositions reported here. The peak amplitude at each pressure and temperature was normalized to reflect the fraction of

reacted HMX for each experiment. Figure 4a shows the fraction reacted as a function of temperature at six different pressures, all at a 0.5 °C/min heating rate; Figure 4b shows the fraction reacted at four different pressures, all at a 0.25 °C/min heating rate. In both figures it is evident there are two regimes with different trends. At relatively low pressures, i.e. between ambient and ca. 1 GPa, raising the pressure lowers the decomposition temperature. At relatively high pressures, i.e. $P > 1$ GPa, raising the pressure raises the decomposition temperature.

As discussed above, at ambient pressure HMX decomposes from the δ -phase whereas at elevated pressures (ca. $P > 0.3$ GPa) HMX decomposes from the β -phase.⁹ In Figures 4a and 4b the phase of HMX undergoing decomposition is clearly labeled and most of the curves represent one phase of decomposition exclusively. However, at relatively low pressures (i.e. between ambient and 1 GPa) HMX can partially decompose in the β -phase (i.e. $\beta \rightarrow$ products reaction) prior to undergoing a phase transformation to the δ -phase, consequently, it is possible to monitor both β - and δ -phase decomposition at the same pressure. Figure 5a shows the peak amplitude for both β - and δ -phase HMX (ca. 3026 cm^{-1} and 3057 cm^{-1} respectively) at 0.08 GPa. In both curves, the β -phase peak amplitude decreases without any change amplitude of the δ -phase peak, this is indicative of a $\beta \rightarrow$ products reaction (which is a multistep reaction, however, our time resolution does not allow investigation of any intermediate steps). At 203 °C the decay of the β -phase peak accelerates and there is a concomitant rise in the amplitude of the δ -phase peak, indicative of a $\beta \rightarrow \delta$ phase transition. The δ -phase lingers briefly and starts to decay, presumably due to the $\delta \rightarrow$ products reaction (which is actually a multistep reaction). The same general trend is observed in Figure 5b at 0.1 GPa, however, the $\beta \rightarrow \delta$ phase transition occurs at a higher temperature (due to the elevated pressure) and is considerably faster. In contrast, Figure 3 shows the ambient pressure curve for β and δ -phase peak amplitude, where it is clear that the $\beta \rightarrow \delta$ phase transformation occurs prior to any decomposition reactions of β -HMX.

In Figure 4a, the 0.08 GPa curve corresponds to the $\beta \rightarrow$ products and $\delta \rightarrow$ products reactions (i.e. exclusively decomposition and no phase transition); the early decomposition is due to β -phase and the

late decomposition is due to δ -phase. The 0.1 GPa curve in Figure 4b underwent a similar decomposition pathway; the demarcation between $\beta \rightarrow$ products and $\delta \rightarrow$ products reactions is at the point where the curve steepens (i.e. 0.35 fraction reacted, 209 °C). Figure 4b also shows a curve labeled <1 GPa (purple curve) in which HMX decomposed exclusively in the β -phase and no δ -phase HMX was ever observed in the experiment. The pressure in this experiment was not well resolved; however, we expect the pressure to be between 0.3 and 1 GPa due to the all β -phase decomposition and the design of the experiment. Most notable about this curve is its shape: decomposition proceeds at a reasonable rate and then, at 213 °C suddenly accelerates and is complete in just a few minutes. It is unlikely that the sudden change in decomposition is due to a pressure vent because one would expect a sudden drop in pressure to halt or slow the decomposition rather than accelerate it. In addition, trapped gases were present and observed to form throughout the experiment and a pressure vent should allow such gases to escape. These curves will be discussed more fully in the discussion section and provide some insight into the role of the polymorph in the decomposition kinetics of HMX.

Kinetic Analysis

Arrhenius based thermal decomposition rates were determined by fitting data from multiple heating rates at the same pressure. A nucleation and growth, global-kinetic-model based on the extended-Prout-Tompkins (e-PT) model^{18,19} was chosen. The e-PT model is shown in equation 1

$$dx/dt = (Ae^{-E/RT})(1-x)^n(1-q(1-x))^m \quad (1)$$

where x is the fraction reacted, E is the activation energy, R is the gas constant, T is temperature, A is the prefactor, n , m , and q are unitless variables associated with the reaction order, autocatalysis and nucleation, respectively. The e-PT model is appropriate for modeling the kinetics of autocatalytic decomposition such as that of HMX.^{5,20} Piermarini et al. used the Avrami-Erofeev model to determine the kinetics of HMX decomposition in their experiments.⁹ Burnham et al. demonstrated that the Avrami-Erofeev and the e-PT models are numerically similar; indicating that the results of our kinetic analysis

can be compared with those of Piermarini et al.²¹ Our data was fit to the e-PT model using the LLNL program Kinetics05²², which numerically integrates the e-PT equation through the exact thermal history.

Due to experimental challenges, reproducing the same pressure to within a few tenths of a GPa in a dynamic decomposition experiment for multiple heating rates is extremely difficult; consequently, our study is limited four key pressure points (ambient pressure, 0.09 GPa, 1.1 GPa, and 3.6 GPa), which are the average pressures of multiple experiments. In the case of the 0.09 GPa data, there was insufficient data for a kinetic analysis of the β -phase, but there was enough data for a kinetic analysis of the δ -phase decomposition. Fits to the raw data are shown in Figures 6-9 and the fit parameters are listed in Table 1. The decomposition rate was calculated at 285 °C and compared with the decomposition rate reported by Piermarini et al.⁹ at the same temperature. The natural log of the decomposition rates at $T = 285$ °C are plotted as a function of pressure in Figure 10. The decomposition rates at 290 and 300 °C were calculated and are reported in the Supporting Information Table S1. These higher temperature rates show a similar overlap with the rates reported by Piermarini et al.⁹

One limitation of the e-PT model is the number of independent variables; one variable could compensate for another in some cases. As such, we fit the data using fixed values of ‘q’ and found only marginal differences in the other parameters. We fixed the value of ‘n’ to 0.5, which is the average value of ‘n’ in the unrestricted fits, and the value of ‘q’ to 0.99, which is the best fit value for ‘q’ in the unrestricted fits, and fit the remaining three parameters (A, E, and m) and found that they were similar to those reported in Table 1 (refer to the Supporting Information Table S2). The kinetic compensation effect outlined by Brill et al.⁵ was tested with our fit parameters by plotting $\ln(A)$ vs. E for every fit (i.e. all pressures; fixed and unrestricted fits). In all cases, our e-PT model results match well with literature values compiled by Brill et al.⁵ and deviated from Brill’s kinetic compensation regression line by only 5-13% (refer to Figure 11). The agreement of our data with the kinetic compensation regression line indicates that the fit parameters and the derived decomposition rates accurately represent the decomposition nature of HMX at the designated pressures.

An analysis of our data was performed using the isoconversional method by Friedman.²³ The isoconversional analysis allows for a calculation of the activation energy (E) and $\ln(Ax^n)$ (A is the Arrhenius prefactor, x is the fraction reacted, n is the reaction order) without assigning a reaction model. The activation energy and $\ln(Ax^n)$ are plotted as a function of fraction reacted at each pressure and are shown in the Supporting Information Figures S1 and S2. The average value for E and $\ln(Ax^n)$ at each pressure is reported in Table 2. In general, the average values represent the decomposition parameters accurately, only the 0.09 GPa data shows any significant fluctuation. Most importantly, the average activation energy shows the same trend and similar values to those calculated using the e-PT model.

A fraction-dependent decomposition rate was calculated using the isoconversional method by assigning a unimolecular decomposition model (i.e. $n = 1$) and a temperature of 285 °C. The average rates are reported in Table 2 and the fraction/pressure-dependent rates are shown in Figure 12. The advantage of this method is that all the pressure dependent data can be compared using a single/identical parameter assumption (i.e. $n = 1$). Both the isoconversional analysis and the e-PT analysis methods produce the same pressure-dependent trend in decomposition rates, however, the actual values are quite different. The $\ln(A)$ vs. E pairs from the isoconversional analysis fit well with Brill's kinetic compensation regression line (refer to Figure 11).⁵

Discussion

The main finding of our high pressure decomposition study is that pressure accelerates HMX decomposition at low to moderate pressures (i.e. ambient up to 1 or 2 GPa) and decelerates decomposition at higher pressures (i.e. greater than ca. 2 GPa). The fractional decomposition curves in Figure 4a clearly shows that the onset of decomposition shifts as a function of pressure: at 0.08 GPa and 1 GPa HMX decomposes at temperatures well *below* the ambient pressure decomposition temperature, at 2.3 GPa and above HMX decomposes at temperatures *above* the ambient pressure decomposition temperature. Two different methods of kinetic analysis of our data indicate that the rate of decomposition accelerates up to 0.09 GPa and decelerates at some pressure above 0.09 GPa (the true

inflection point may not be 0.09 GPa but given our range of data points 0.09 GPa is a reasonable approximation of the true inflection point). Comparison of our e-PT decomposition rates with literature values by Burnham et al.^{8,24} and Piermarini et al.⁹ show excellent agreement, as is shown in Figure 10 and Table 1. Neither Burnham nor Piermarini's study was able to show this inflection in the pressure dependent decomposition kinetics because the two studies investigated different pressure regimes, employed different methods (DSC vs. DAC), and different polymorphs of HMX (δ vs. β). However, these studies in combination with our work irrefutably demonstrate this pressure dependent trend in the decomposition kinetics of HMX and strengthen each study's conclusions.

The change in the decomposition kinetics, in particular the pressure dependent change from acceleratory to deceleratory, is attributed to two different mechanisms driving the decomposition kinetics. It is well established that at ambient pressure, the decomposition of HMX involves heterogeneous, autocatalytic reactions, i.e. reactive gases, which are produced through the breakdown of HMX, accelerate the decomposition of starting material and transient species.^{5,20,25} It is also well established that pressure will increase the collision frequency of gaseous species and hence accelerate gas-phase and heterogeneous reactions.²⁶ We hypothesize that the acceleration in HMX decomposition, up to 0.09 GPa, is due to the enhancement of these heterogeneous and autocatalytic reactions.

The deceleration of HMX decomposition at higher pressures is attributed to pressure hindering the decomposition initiation step. In a study by Naud and Brower,¹ HMX was dissolved in acetone and the decomposition rate of HMX was monitored at various pressures ranging from ambient to 100 MPa. Dissolving the HMX in acetone inhibited intermolecular reactions and quenched the reactive transient species (e.g. NO_2), hence Naud and Brower were able to monitor the initiation steps in decomposition without the complications of heterogeneous and autocatalytic reactions. Their study clearly shows that pressure hinders and decelerates decomposition between ambient and 100 MPa. They concluded that the first step in the decomposition of HMX has a positive activation volume and they hypothesized that the reaction begins with HONO elimination and/or N-NO_2 bond homolysis. Taking into consideration

the results of Naud and Brower's work, it seems most likely that the deceleration in HMX decomposition we observe in our solid state study is also due to pressure hindering the initiation step(s).

We expect that the competing effects of pressure on the decomposition of HMX are occurring over the full range of pressures in our study; however, one mechanism dominates over the other at different pressure regimes. As one raises the pressure, the initial decomposition of HMX is hindered, however, a sufficient population decomposes resulting in reactive gases which accelerate the decomposition, and the rate is determined by the degree of autocatalysis. At the true inflection point pressure hinders the initiation step so much that the rate is determined by the rate of HONO and/or N-NO₂ bond homolysis.

The role and influence of the HMX polymorph in the decomposition kinetics of HMX is a more difficult topic of study because the decomposition is complex and decomposing β and δ -phase HMX under similar conditions is difficult. Figure 4a and 4b show β and δ phase decomposition of HMX at low pressures (i.e. < 1 GPa). In the experiments at ca. 0.08 and 0.1 GPa the sample begins to decompose in β -phase, then undergoes a rapid and complete phase transformation to δ -phase, and completes decomposition from the δ -phase. There was insufficient data for a kinetic analysis of the β -phase, but there was enough data for a kinetic analysis of the δ -phase decomposition. Kinetic analysis using the extended Prout-Tompkins method clearly indicates that the δ -phase decomposition at 0.09 GPa is faster than the β -phase decomposition at 1.1 GPa, yet relative to the decomposition at ambient pressure or 3.6 GPa both are quite fast. One should take care, however, in relying too heavily on this quantitative data from the 0.09 GPa δ -phase decomposition, because the reaction was quite fast and only about 15 data points/curve were used to analyze the kinetics. Kinetic analysis using the isoconversional analysis indicates that all of the decomposition parameters (i.e. activation energy, $\ln(Ax^n)$, and rate) of δ -phase HMX at 0.09 GPa are similar to, but considerably more variable, than that of β -phase HMX at 1.1 GPa. More work is necessary in order to draw any firm and quantitative conclusions about the kinetics of β - versus δ -phase HMX.

In addition to a quantitative comparison, a qualitative analysis provides some insight into the relative decomposition rates of β - vs. δ -phase. Comparison of the shape of the β and δ -phase decomposition curves at 0.08 and 0.1 GPa is interesting (see Figure 4). In both experiments, the β -phase curve has a gentle slope and the δ -phase curve has a very steep slope. This may indicate that in these two experiments, δ -phase decomposes faster than β -phase, yet the <1 GPa curve in Figure 4b shows a similar change in slope when the sample decomposed exclusively in the β -phase. It is possible that the sudden change in slope in the <1 GPa curve results from a rapid and sequential $\beta \rightarrow \delta \rightarrow \text{product}$ decomposition mechanism, where the δ -phase may be unobservable due to our ca. 1 minute time resolution. It is also possible that the acceleration is due to enhanced autocatalysis and not a change in mechanism or an inherent change in the chemical kinetics of one phase vs. the other. The data presented here is insufficient to make a definitive statement about whether β - or δ -phase HMX decomposes more rapidly under identical conditions, however, the results clearly indicate that both polymorphs are sensitive to pressure during thermal decomposition.

Summary

The results of this study further elucidate the pressure dependent thermal decomposition process starting from β - or δ -phase HMX. A decomposition rate inflection point was found in the 100 MPa regime. The decomposition rate dependence on pressure is attributed, though not limited to, the competing effects of autocatalysis, which is enhanced with pressure, and reaction initiation, which is hindered by pressure. These results allow for a more confident assessment of thermal safety of HMX based materials and will guide in the interpretation of multivariable cook-off experiments. Further work is underway to investigate some of the remaining questions concerning the pressure dependent decomposition kinetics of HMX.

ACKNOWLEDGMENT

We thank J.L. Maienschein for helpful discussion and Sabrina DePiero for supplying the samples. This work performed under the auspices of the U.S. Department of Energy by Lawrence Livermore National Laboratory under Contract DE-AC52-07NA27344.

Supporting Information Available

Prout-Tompkins based reaction rates at different temperatures and model fit parameters with fixed values for 'n' and 'q', isoconversional analysis results (E and $\ln(Ax^n)$) of HMX decomposition. This information is available free of charge via the Internet at <http://pubs.acs.org>.

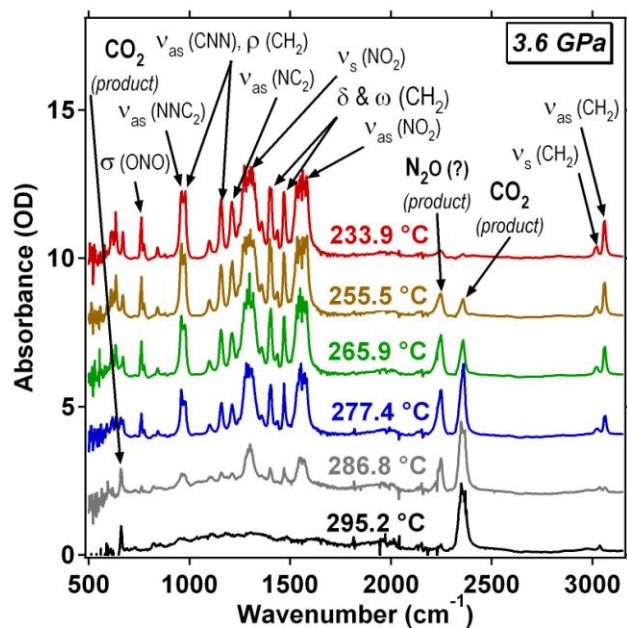


Figure 1. Infrared absorption spectra for β -HMX decomposition at 3.6 GPa during a ramped heating experiments (0.5 °C/min). Spectra baselines were vertically shifted for easy visualization.

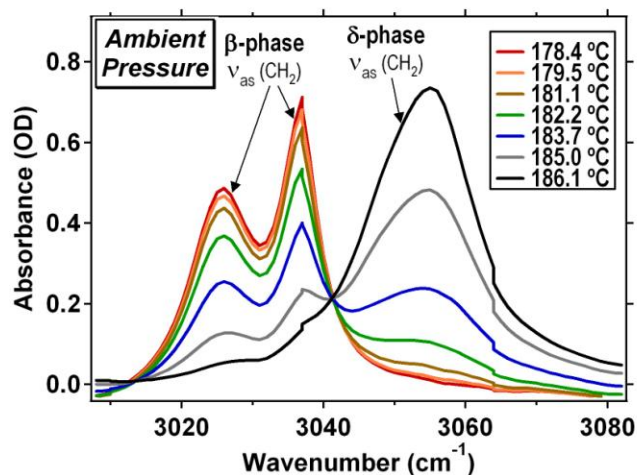


Figure 2. Infrared absorption spectra showing the conversion of β -phase HMX to δ -phase at ambient pressure during a ramped heating experiments (0.5 °C/min).

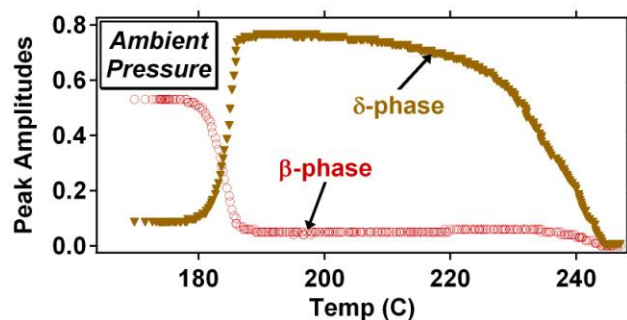


Figure 3. Infrared peak amplitude for the 3026 and 3055 cm^{-1} peaks (asymmetric CH_2 stretch of HMX in β - and δ -phase respectively) at ambient pressure during a ramped heating experiments (0.5 $^{\circ}\text{C}/\text{min}$).

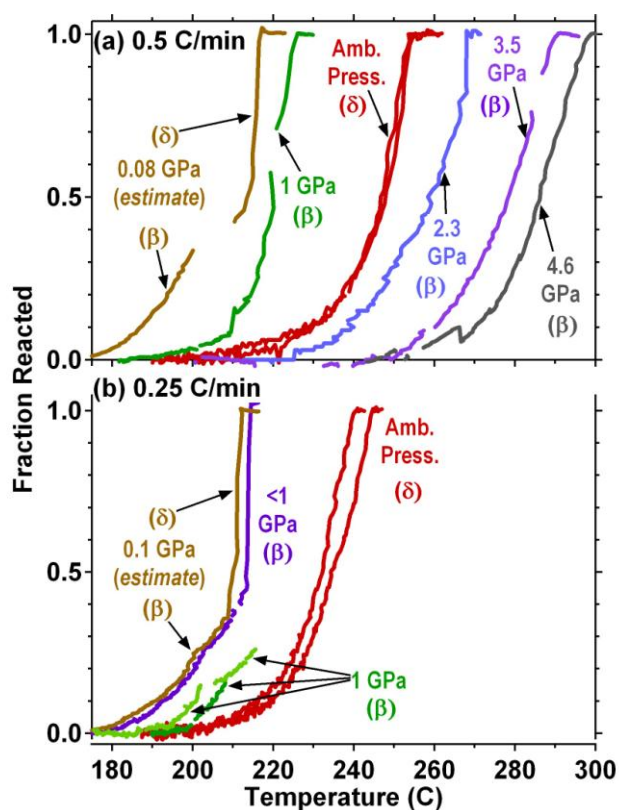


Figure 4. Fraction of HMX decomposed at various pressures at (a) 0.5 $^{\circ}\text{C}/\text{min}$ heating rate and (b) 0.25 $^{\circ}\text{C}/\text{min}$ heating rate. The phase/polymorph of HMX (β or δ) is labeled for each curve. In the case of the 0.08 GPa and 0.1 GPa decomposition, HMX began to decompose in β -phase, then underwent β - δ phase transition and completed the decomposition in δ -phase. At all other pressures, the decomposition was exclusively in a single phase.

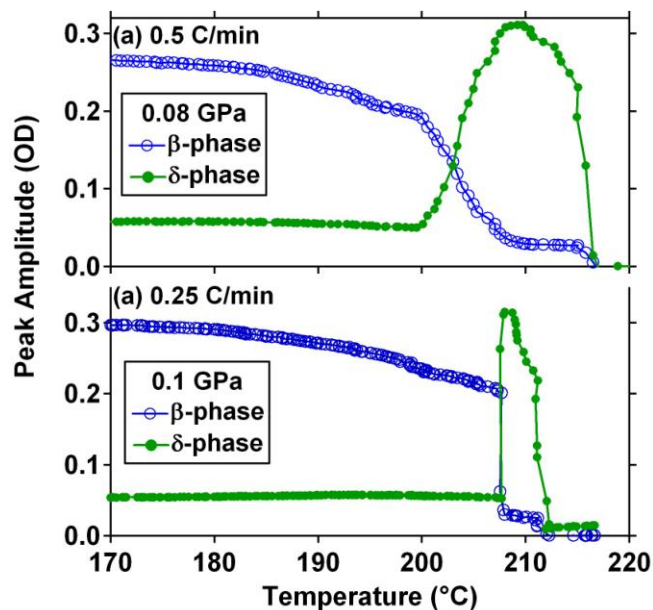


Figure 5. Peak amplitude of β - and δ -phase HMX at 0.08 and 0.1 GPa. The initial decay of β -HMX (with no corresponding rise of δ -HMX) is attributed to $\beta \rightarrow$ product reaction. The concomitant decay of β -HMX and rise of δ -HMX corresponds to the $\beta \rightarrow \delta$ phase transition. The decay of δ -HMX is attributed to the $\delta \rightarrow$ product reaction. The $\beta \rightarrow$ product and $\delta \rightarrow$ product reactions were used to construct the orange curves in Figure 4.

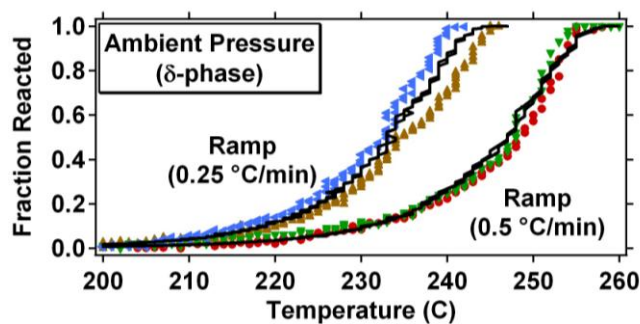


Figure 6. Kinetic model fits (black lines) to the raw data (colored points) corresponding to ambient pressure, δ -phase decomposition of HMX.

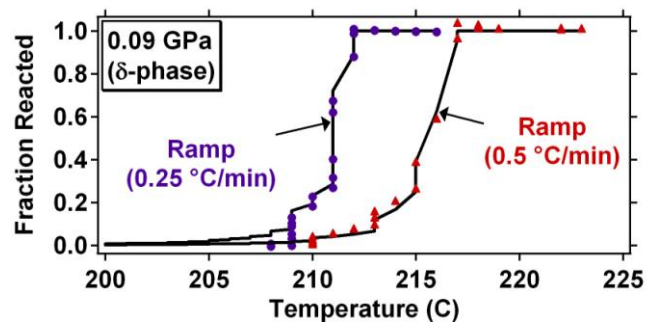


Figure 7. Kinetic model fits (black lines) to the raw data (colored points) corresponding to 0.09 GPa δ -phase decomposition of HMX. Note that both sets of data originate from experiments where the sample began to decompose in β -phase and underwent a $\beta \rightarrow \delta$ phase change and completed decomposition in δ -phase (refer to figure 4). The data shown here corresponds to the fraction of δ -phase decomposition only and not the total HMX decomposition (i.e. β -phase decomposition is excluded).

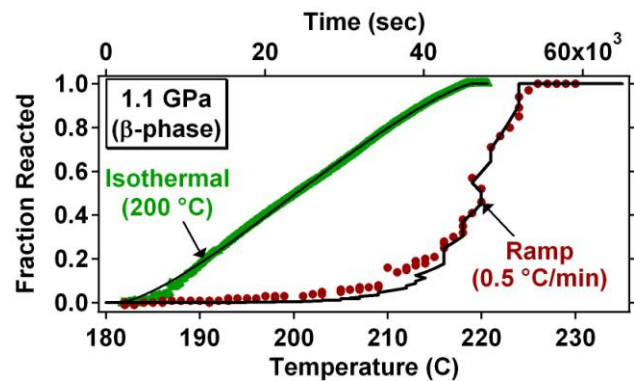


Figure 8. Kinetic model fits (black lines) to the raw data (colored points) corresponding to 1.1 GPa, β -phase decomposition of HMX.

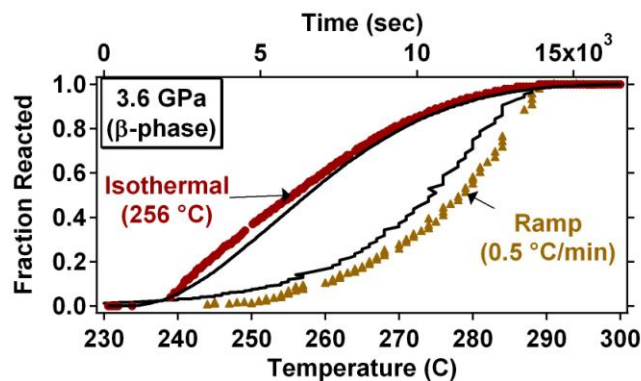


Figure 9. Kinetic model fits (black lines) to the raw data (colored points) corresponding to 3.55 GPa, β -phase decomposition of HMX.

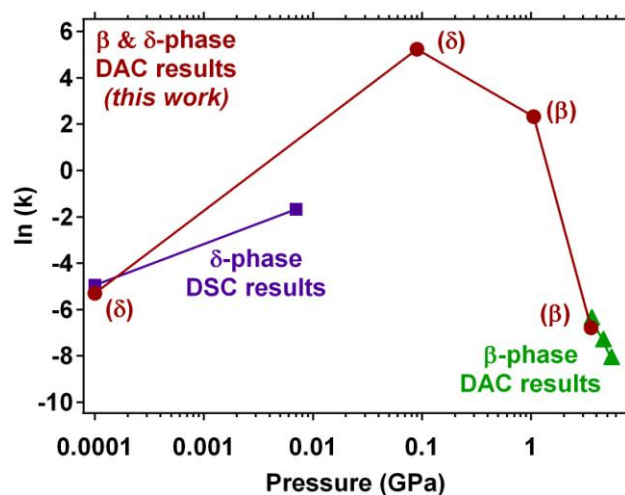


Figure 10. Pressure dependent reaction rates for HMX decomposition. Red circles correspond to DAC results from this work. Purple squares correspond to DSC results presented by Burnham et al.^{8,24} and green triangles correspond to DAC results presented by Piermarini et al.⁹ Lines are guides to the eye. All rates correspond to the Arrhenius rate calculated at 285 °C based on the activation energy and Arrhenius prefactor determined from the extended Prout-Tompkins method. See Table 1 for all Prout-Tompkins values.

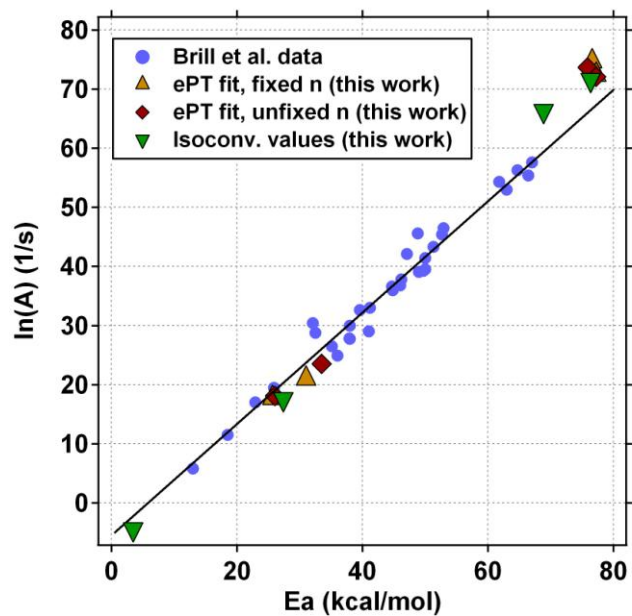


Figure 11. HMX thermal decomposition kinetic compensation plot. Brill et al. data from Table 1 in reference ⁵.

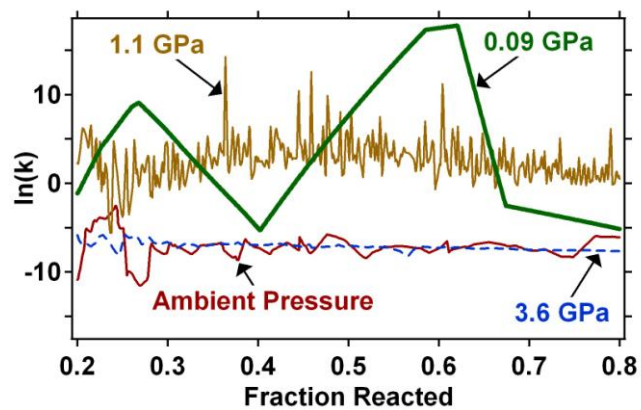


Figure 12. Pressure dependent reaction rates for HMX decomposition based on the isoconversional analysis assuming unimolecular decomposition at $T = 285\text{ }^{\circ}\text{C}$. See Table 2 for the complete isoconversional analysis results.

Table 1. Kinetic model fit parameters for HMX decomposition at various pressures using the extended-Prout-Tompkins global kinetic model.

Pressure (GPa)	k (1/s) ^a	A (1/s) ^b	E (kcal/mol) ^b	m ^b	n ^b	q ^b	Expt. Method ^c	Phase of HMX	Ref.
1. 0E-04	0.0079	5.50E+10	32.9	0.25	0.51	0.9999	DSC	δ	d
7. 0E-03	0.2108	2.83E+12	33.6	1.19	0.77	0.9999	DSC	δ	e
1.0E-04	0.0050	7.31E+07	26.1	0.64	0.41	0.99	DAC	δ	this work
0.09	185.80	9.94E+31	75.9	1.26	0.34	0.99	DAC	δ	this work
1.1	10.857	1.96 E+31	77.3	0.31	0.26	0.99	DAC	β	this work
3.6	0.0012	1.61 E+10	33.5	0.46	0.64	0.99	DAC	β	this work
3.6	0.0016	NA	NA	NA	NA	NA	DAC	β	f
4.6	0.0006	NA	NA	NA	NA	NA	DAC	β	f
5.5	0.0003	NA	NA	NA	NA	NA	DAC	β	f

^a Global decomposition rate calculated using the Arrhenius equation at a temperature of 285 °C.

^b Model parameters for the extended Prout-Tompkins model: $dx/dt = (Ae^{-E/RT})(1-x)^n(1-q(1-x))^m$ where x is the fraction reacted, E is the activation energy, R is the gas constant, T is temperature, A is the pre-factor, n, m, and q are unitless variables associated with the reaction order, autocatalysis and nucleation, respectively.

^c DSC = differential scanning calorimetry; DAC = diamond anvil cell

^d Reference 24

^e Reference 8

^f Decomposition rate estimated from figure 8 of reference 9

Table 2. The average kinetic parameters for HMX decomposition at various pressures using the Friedman isoconversional analysis; all values are averaged between the fraction reacted range of 0.2 and 0.8.

Pressure (GPa)	E (kcal/mol) ^a	ln(Axⁿ) ^a	k (1/s) ^b	A (1/s) ^c	Expt. Method ^d	Phase of HMX
1.0E-04	3.4	-4.8	2.26E-03	9.98E+16	DAC	δ
0.09	68.9	65.3	3.16E+06	1.38E+75	DAC	δ
1.1	76.4	70.7	5.70E+04	6.07E+79	DAC	β
3.6	27.4	16.8	8.87E-04	3.00E+14	DAC	β

^a Parameters for Friedman isoconversional analysis; E is the activation energy, A is the Arrhenius prefactor, x is the fraction reacted and n is the reaction order. Refer to Supporting information Figures S1 and S2 for complete data sets.

^b Decomposition rate calculated using the Arrhenius equation at a temperature of 285 °C and assigning a reaction order of n = 1.

^c Arrhenius prefactor calculated with a reaction order of n = 1.

^d DAC = diamond anvil cell

Table S1. Extended-Prout-Tompkins based reaction rates at different temperatures.

Pressure (GPa)	k (1/s) ^a T = 290 °C	k (1/s) ^a T = 300 °C	Expt. Method ^b	Phase of HMX	Ref.
1. 0E-04	9.2E-03	9.2E-03	DSC	δ	c
7. 0E-03	2.5E-01	2.5E-01	DSC	δ	d
1.0E-04	5.6E-03	8.4E-03	DAC	δ	this work
0.09	3.4E+02	1.1E+03	DAC	δ	this work
1.1	2.0E+01	6.7E+01	DAC	β	this work
3.6	1.6E-03	2.6E-03	DAC	β	this work
3.6	4.6E-03	6.7E-03	DAC	β	e
4.6	1.2E-03	1.4E-03	DAC	β	e
5.5	5.6E-04	1.1E-03	DAC	β	e

^a Global decomposition rate calculated using the Arrhenius equation at designated temperature. Rates based on Arrhenius parameters from extended Prout-Tompkins model, see Table 1.

^b DSC = differential scanning calorimetry; DAC = diamond anvil cell

^c Reference 24

^d Reference 8

^e Decomposition rates estimated from figure 8 of reference 9

Table S2. Kinetic model fit parameters for HMX decomposition at various pressures using the extended-Prout-Tompkins global kinetic model with ‘n’ restricted to a value of 0.5 and ‘q’ restricted to 0.99.

Pressure (GPa)	k (1/s)^a	A (s⁻¹)^a	E (kcal/mol)^a	m^a	n^a	q^a	Expt. Method^b	Phase of HMX
1.0E-04	0.0043	4.87E+07	25.7	0.56	0.50	0.99	DAC	δ
0.09	258.15	2.66E+32	76.6	1.33	0.50	0.99	DAC	δ
1.1	14.865	2.70E+31	77.3	0.44	0.50	0.99	DAC	β
3.6	0.0009	1.26E+09	31.0	0.42	0.50	0.99	DAC	β

^a Model parameters for the extended Prout-Tompkins model: $dx/dt = (Ae^{-E/RT})(1-x)^n(1-q(1-x))^m$ where x is the fraction reacted, E is the activation energy, R is the gas constant, T is temperature, A is the pre-factor, n, m, and q are unitless variables associated with the reaction order, autocatalysis and nucleation, respectively.

^b DAC = diamond anvil cell

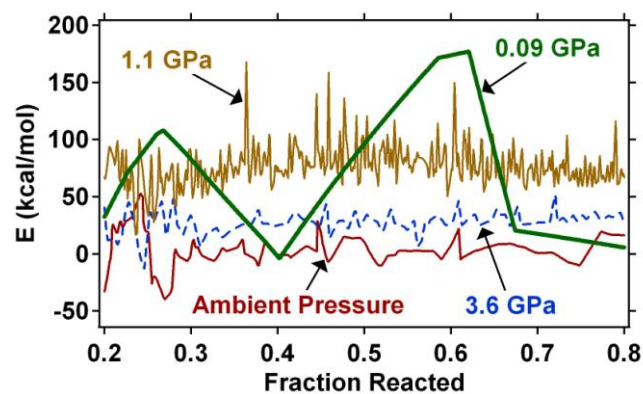


Figure S1. Activation energy for HMX decomposition based on the isoconversional analysis.

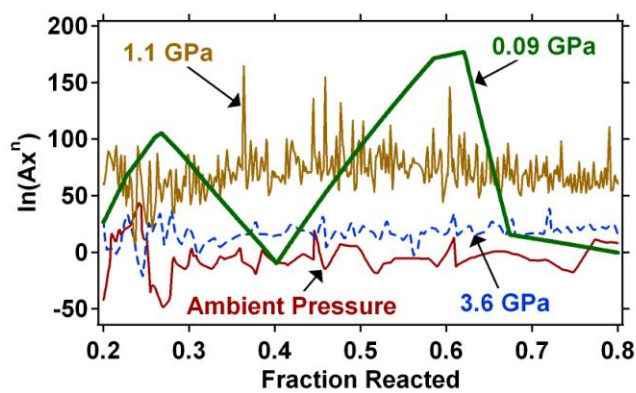


Figure S2. Isoconversional analysis results of HMX decomposition at various pressures.

REFERENCES (Word Style “TF_References_Section”).

- (1) Naud, D. L.; Borower, K. R. J. Org. Chem. 1992, 57, 3303.
- (2) Chakraborty, D.; Muller, R. P.; Dasgupta, S.; Goddard III, W. A. J. Phys. Chem. A 2001, 105, 1302.
- (3) Behrens Jr., R. Thermal Decomposition Processes of Energetic Materials in the Condensed Phase at Low and Moderate Temperatures. In Overviews of Recent Research on Energetic Materials; Shaw, R. W., Brill, T. B., Thompson, D. L., Eds.; World Scientific Publishing Co. Pte. Ltd.: Hackensack, NJ, 2005.
- (4) Oyumi, Y.; Brill, T. B. Combustion and Flame 1985, 62, 213.
- (5) Brill, T. B.; Gongwer, P. E.; Williams, G. K. J. Phys. Chem. 1994, 98, 12242.
- (6) Tarver, C. M.; Tran, T. D. Combustion and Flame 2004, 137, 50.
- (7) Wemhoff, A. P.; Howard, M. H.; Burnham, A. K.; Nichols III, A. L. J. Phys. Chem. A 2008, 112, 9005.
- (8) Burnham, A. K.; Weese, R. K.; Wardell, J. F.; Tran, T. D.; Wemhoff, A. P.; Koerner, J. G.; Maienschein, J. L. 13th International Detonation Symposium, Norfolk, VA, Office of Naval Research, 2006,573.
- (9) Piermarini, G. J.; Block, S.; Miller, P. J. J. Phys. Chem. 1987, 91, 3872.
- (10) Henson, B. F.; Smilowitz, L.; Asay, B. W.; Sandstrom, M. M.; Romero, J. J. 13th Int. Det. Symp., Norfolk, VA, Office of Naval Research, 2006,778.

- (11) Lee, E. R.; Sandborn, R. H.; Stromberg, H. D. Proc. 5th Symp. (Int) Detonation, Pasadena, CA, Office of Naval Research, 1970,331.
- (12) Maienschein, J. L.; Wardell, J. F.; DeHaven, M. R.; Black, C. K. Propellants, Explosives, Pyrotechnics 2004, 29, 287.
- (13) Wardell, J. F.; Maienschein, J. L. 12th Int. Det. Symp., San Diego, CA, Office of Naval Research, 2002,384.
- (14) Datchi, F.; LeToullec, R.; Loubeyre, P. J. Appl. Phys. 1997, 81, 3333.
- (15) Montgomery, W.; Zaug, J. M.; Howard, M. H.; Goncharov, A. F.; Crowhurst, J. C.; Jeanloz, R. J. Phys. Chem. B 2005, 109, 19443.
- (16) Landers, A. G.; Brill, T. B. J. Phys. Chem. 1980, 84, 3573.
- (17) Brand, H. V.; Rabie, R. L.; Funk, D. J.; Diaz-Acosta, I.; Pulay, P.; Lippert, T. K. J. Phys. Chem. B 2002, 106, 10594.
- (18) Burnham, A. K.; Braun, R. L. Energy and Fuels 1999, 13, 1.
- (19) Burnham, A. K.; Weese, R. K.; Wemhoff, A. P.; Maienschein, J. L. Journal of Thermal Analysis 2007, 89, 407.
- (20) Behrens Jr., R.; Margolis, S. B.; Hobbs, M. L. 11th International Detonation Symposium, Snowmass, CO, Office of Naval Research, 1998,533.
- (21) Burnham, A. K.; Braun, R. L.; Coburn, T. T.; Sandvik, E. I.; Curry, D. J.; Schmidt, B. J.; Nobel, R. A. Energy and Fuels 1996, 10, 49.
- (22) Kinetics05, Braun, R. L.; Burnham, A. K.; The Regents of the University of California: Livermore, CA, 2006.

- (23) Friedman, H. L. J. of Polymer Sci. Part C 1964, 6, 183.
- (24) Burnham, A. K.; Weese, R. K. 36th Intl. ICT conference and 32nd Intl Pyrotechnics Seminar, Karlsruhe, Germany, 2005,1.
- (25) Behrens Jr., R.; Bulusu, S. Fourth International Symposium on Special Topics in Propulsion, 1996,278.
- (26) McQuarrie, D. A.; Simon, J. D. Physical Chemistry: A Molecular Approach; University Science Books: Sausalito, CA, 1997.